Concentration Gradient Immunoassay. 1. An Immunoassay Based on Interdiffusion and Surface Binding in a Microchannel

ARTICLE *in* ANALYTICAL CHEMISTRY · JUNE 2007

Impact Factor: 5.64 · DOI: 10.1021/ac062349w · Source: PubMed

3 AUTHORS, INCLUDING:

Kjell Nelson
University of Maryland, College Park
16 PUBLICATIONS **1,550** CITATIONS
SEE PROFILE

Paul Yager
University of Washington Seattle
214 PUBLICATIONS **8,226** CITATIONS
SEE PROFILE

Published in final edited form as:
Anal Chem. 2007 May 15; 79(10): 3542–3548. doi:10.1021/ac062349w.

Concentration Gradient Immunoassay I. A Rapid Immunoassay Based on Interdiffusion and Surface Binding in a Microchannel

Kjell E. Nelson, **Jennifer O. Foley**, and **Paul Yager***
Department of Bioengineering, University of Washington, Seattle, WA 98195

Abstract

We describe a novel microfluidic immunoassay method based on the diffusion of a small molecule analyte into a parallel-flowing stream containing cognate antibody. This interdiffusion results in a steady-state gradient of antibody binding site occupancy transverse to convective flow. In contrast to the diffusion immunoassay (Hatch et al. *Nature Biotechnology*,19:461−465 (2001)), this antibody occupancy gradient is interrogated by a sensor surface coated with a functional analog of the analyte. Antibodies with at least one unoccupied binding site may specifically bind to this functionalized surface, leading to a quantifiable change in surface coverage by the antibody. SPR imaging is used to probe the spatial distribution of antibody binding to the surface and, therefore, the outcome of the assay. We show that the pattern of antibody binding to the SPR sensing surface correlates with the concentration of a model analyte (phenytoin) in the sample stream. Using an inexpensive disposable microfluidic device, we demonstrate assays for phenytoin ranging in concentration from 75 to 1000 nM in phosphate buffer. At a total volumetric flow rate of 90 nL/sec, the assays are complete within 10 minutes. Inclusion of an additional flow stream on the side of the antibody stream opposite to that of the sample enables simultaneous calibration of the assay. This assay method is suitable for rapid quantitative detection of low-molecular weight analytes for point-of-care diagnostic instrumentation.

Keywords

microfluidics; immunoassay; surface plasmon resonance; point-of-care diagnostics

INTRODUCTION

The development of automated, point-of-care diagnostic instrumentation promises to dramatically improve patient care and may ultimately lead to “individualized” patient therapy regimens, particularly for those patients undergoing treatment with drugs with rapid pharmacokinetics and narrow therapeutic ranges.

Three primary factors need to be considered when developing such a system: a rugged, inexpensive analytical device; assays that are rapid, accurate, and quantitative; and a sample fluid that is easy and comfortable to collect that provides meaningful clinical data. Such a system is likely to consist of two parts: an automated reader and a disposable “card” that a can be loaded with a small sample of fluid and inserted into the reader by a non-expert user [1].

Surface plasmon resonance (SPR) is a particularly attractive detection technology for low-cost point-of-care testing as it does not require labeled reagents, the instrument components are relatively simple and inexpensive, the power requirements are modest; also, the potential for developing miniature SPR devices is largely untapped[2-10]. Imaging-based SPR sensing

*To whom correspondence should be addressed: e-mail – yagerp@u.washington.edu.

(SPRI) can extend this already sensitive and widely adopted detection method to more sophisticated, spatiotemporal pattern-based assay methodologies, including multiple simultaneous measurements of different targets, as well as calibrants for positive and negative controls.

Microfluidics (and its integration into what is known as Lab-on-a-Chip) is a key enabling technology for point-of-care diagnostics as it promises improvements over standard immunoassay formats in terms of speed, sensitivity and reagent consumption, and can potentially be highly automated[11-20]. A low-cost disposable microfluidic card could, in principle, carry out the necessary tests using a small patient sample and a scant amount of expensive reagents, (such as antibodies). Ideally, these immunoassays would have comparable sensitivity to currently used ELISA conducted in standard 96-well format, despite being carried out in significantly less time.

The selection of a sample fluid that will enable frequent, meaningful measurements, ideally by an untrained user (such as the patient) will be a key factor in the success of such a system in a point-of-care setting. A number of sample fluids are available, including blood, urine, stool and saliva. Of these, saliva is by far the most easily and comfortably collected. To date, however, there are relatively few saliva-based tests available, particularly compared to those available for blood products.

Saliva is a largely underutilized sample fluid for a variety of reasons, not the least of which is a perception on the part of clinicians that it is inferior to blood with respect to the correlation of salivary analyte concentrations with clinically established blood levels that are now almost exclusively used to make therapeutic decisions. However, for those clinical analytes that are small and non-polar and can freely diffuse across the epithelium of the acinar cells in the salivary ducts, strong correlations to free plasma levels have been shown to exist[21]. Moreover, perceptions are beginning to change regarding the use of saliva as a sample fluid[22, 23], and few could argue against the fact that frequent home testing would be greatly facilitated by the ability to use saliva due to its ease of collection[21, 22, 24]. The development of assays that are capable of reliably detecting clinically meaningful levels of analytes in saliva will encourage the widespread acceptance of saliva for diagnostic monitoring.

While non-polar, low molecular weight analytes can be highly correlated with free plasma levels and therefore are good initial targets for the development of a saliva-based, point-of-care diagnostic instrument, low molecular weight analytes are difficult to detect directly using SPR. Indirect immunoassay methods based on interaction between the target and a label could be more suitable, provided that the “label” leads to a strong enough signal for sensitive detection with SPR. Sandwich immunoassay formats are not suitable for detecting low molecular weight analytes since the target is typically not large enough to present more than one epitope to binding antibodies. Developing indirect competitive immunoassays for detecting low molecular weight analytes using SPR imaging on microfluidic platforms is an important step toward the development of rapid, affordable point-of-care diagnostic testing and therapeutic drug monitoring. To date, however, very little work has been done toward this goal. To fill this gap, we describe here a novel immunoassay method—the competition gradient immunoassay—that is capable of direct measurement of low-molecular weight analytes in less than 10 minutes with simultaneous controls on a single fluid sample. It does not require mixing or labeled reagents. This paper describes the theory of operation of the CGIA and presents initial results obtained using a model low molecular weight analyte, phenytoin. A companion paper presents results obtained from full 3-D computational modeling of the assay method[25]. Future work will describe the operation of this assay for quantitative detection of low molecular weight analytes in physiological fluids such as saliva.

Theoretical Basis

Three main concepts underlie the operation of the CGIA: 1) Fluid flow in microchannels is laminar and dominated by viscous forces (i.e., is devoid of chaotic, turbulent mixing)[20, 26, 27], 2) in the absence of chaotic mixing, mass transport of solutes between miscible fluids occurs only by diffusion and is governed by Fick's Laws, and 3) surface plasmon resonance is only sensitive to changes in refractive index that occur within ~300 nm of the sensor surface [28].

These three concepts are combined and utilized in the device schematically illustrated in Figure 1. The device itself has the following principal features:

1. a microfluidic channel with multiple inlets converging into a single common duct,
2. a "pre-binding" zone of defined length downstream of the fluid convergence points; the channel surface in this zone is functionalized with a PEG-functionalized alkylthiol self-assembled monolayer to reduce depletion of proteins from the fluid via non-specific surface adsorption[29],
3. a SPRI sensor surface that has been specifically functionalized to present an analog of the target compound to molecules in the bulk solution.

The device is operated by flowing the following solutions into one of the three device inlets:

a. the sample, containing an unknown quantity of a relatively rapidly diffusing analyte;
b. an antibody solution specific to the analyte; and
c. (optionally) a reference or control stream with a known concentration of analyte (Figure 1)[1]. For the purposes of this discussion, the control stream will contain buffer only (i.e., the analyte concentration in the control stream is zero).

Due to the laminar fluid flow within the channel, mass transport of molecules across the stable flow lines is determined by diffusion. Therefore, mass flux across the fluid interfaces is determined by the diffusion coefficients of the solutes and their relative concentrations in the adjacent streams. In this case, because the diffusion of small molecule analytes is generally an order of magnitude faster than that of IgG molecules [30], mass transfer is essentially limited to movement of the analyte from the sample into the antibody stream. As the fluid flow rate remains constant during the course of the experiment, a steady-state analyte concentration gradient is established transverse to the convective flow. This flux of analyte into the center stream leads to a gradient of analyte-specific antibody binding site occupancy within the antibody stream near the sample interface (Figure 1b). This antibody binding site occupancy gradient will broaden transverse to flow with increasing channel distance downstream of the fluid entry points, as controlled by the flow rate and the analyte diffusion coefficient.

At a selected distance downstream, the solutions encounter the SPR sensing surface. Recall that this region of the channel surface is coated with a surface-bound analog of the analyte, so that antibodies *having at least one open binding site* may bind to the surface. Binding of a large molecule such as IgG leads to a strong, quantifiable SPR signal change (Figure 1c). In proportion to the flux of the analyte into the antibody stream, the rate of antibody accumulation to the sensor surface near the sample interface will be reduced compared to the rate observed

[1]To facilitate description of this assay, the following terminology will be adopted: the fluid interface on the left (c.f. Fig. 1), defined as the interaction zone between the sample and the antibody streams, will be referred to as the "sample interface"; the fluid interface on the right, between the antibody and control streams, will be referred to as the "control interface". The accumulation of antibody on the SPR sensor surface under flow leads to a "streak" of antibody (observed as a bright band in the SPR difference images (Fig. 4) with two "edges", one on the "competitor side" (to the left of the channel centerline) and one on the "control side" (to the right of the channel center line).

near the control interface. If the analyte concentration is high relative to the concentration of antibody, binding near the sample interface will be completely inhibited.

Thus, the presence of analyte in the sample stream will narrow the width of the sensor surface area to which antibody accumulates compared to what it would be in the absence of analyte. This difference is referred to as the "assay shift" (Figure 1, Figure **4** and Figure **5**). Since Fick's Law dictates that the diffusive flux is proportional to the concentration, for a given antibody concentration the assay shift is related to the concentration of the analyte in the sample solution. This is how the SPR signal change can be used to calculate the concentration of analyte in the sample.

In this paper, we demonstrate this assay principle experimentally using phenytoin (Dilantin) as a model analyte. Phenytoin (FW 252.3) is a small molecule commonly used in the treatment of epilepsy, and is suitable for therapeutic monitoring using saliva as a sample fluid[31]. This will establish the basis for future work demonstrating the rapid, quantitative detection of small molecule analytes in an appropriately preconditioned human saliva sample (filtered, for instance, to remove gross interferents and to reduce its viscosity (K. Helton, personal communication]).

EXPERIMENTAL METHODS

Substrate preparation and surface patterning

The sensing surface of the microfluidic devices used in these experiments consisted of a soda lime glass microscope slide with 45 nm gold/ 1 nm of chromium for an adhesion layer deposited on top by e-beam evaporation (~10^{-6} Torr base pressure, deposition rate ~0.15 nm/sec, 99.999% purity Au). This gold surface is required as it serves as the SPR conductive layer. As illustrated in Figure 1, two different surface treatments were applied to different areas of the channel surface: one to prevent protein adsorption, the other to provide for specific binding of antibodies from solution to the SPR sensor. To minimize protein adsorption, the pre-binding region area of the channel surface was exposed to a PEG-terminated alkylthiol (Prochimia, Sopot, Poland). The SPR sensing area (> 22 mm downstream of the fluid convergence points) was functionalized with a BSA-phenytoin conjugate (Fitzgerald Industries International, Inc., Concord, MA). A linear boundary between the PEG and BSA-conjugate regions that was orthogonal to convective flow was desired to ensure that the total distance from the fluid inlets across the channel cross-section was identical when the solutions reached the sensing area. This surface patterning was accomplished by a method that utilizes capillary forces to spread small volumes of solutions under a Mylar or PMMA "mask" that covered the appropriate area of the surface.

As the different solutes required incompatible solvents (ethanol for the PEG thiol, buffered aqueous solution for the BSA-phenytoin), this surface patterning was done sequentially. First, a solution of PEG thiol (5 mM in ethanol) was spread under a PMMA mask that covered the channel inlets and pre-binding area. Capillary wetting caused the solution to fill the thin gap between the mask and the substrate, stopping at the edges of the mask. The solvent was allowed to evaporate at ambient conditions. This treatment was repeated once to ensure thorough coverage of the non-fouling layer. The mask was then removed from the substrate and any excess thiol was rinsed away under a stream of absolute ethanol. Next, a mask covering the channel surface "downstream" of the PEG coating was placed over the slide. A solution of BSA-phenytoin (10 mg/mL in 25 mM phosphate buffer, pH 8.0) was spread under the mask, again using capillary forces to fill the volume between the mask and the substrate. The BSA-phenytoin solution was allowed to incubate overnight at 4°C in a humidified atmosphere. Finally, the mask was carefully removed and the excess protein rinsed off the surface with

deionized water. The slide was thoroughly blown dry with N_2. If not used immediately, the patterned slides were stored at 4°C under N_2 and used within a week.

Microfluidic device assembly

The microfluidic devices used in these experiments were assembled from poly(ethylene terephthalate) (PET, Mylar™) or poly(methyl methacrylate) (PMMA) sheets (Fralock Inc., San Carlos, CA) laminated together as shown in Figure 2. The device layers consisted of (from bottom to top): 1) substrate (pre-patterned as described above); 2) channel—a 12 μm-thick Mylar™ sheet coated on both sides with 25 μm-thick pressure sensitive adhesive, featuring a 3.6 mm wide channel laser-cut from the center, creating a duct with 3.6 mm × 62 μm average cross-sectional area, approximately 45 mm long; 3) channel cap—a 25 μm thick Mylar™ sheet coated on top with adhesive, featuring vias over the inlets and outlet to permit fluid flow; 4) O-ring seat—a 2.5 mm thick PMMA slab featuring holes over the inlets and outlet to retain ethylene propylene diene monomer rubber (EPDM) o-rings, and 5) O-ring retainer—a 25 μm thick Mylar™ sheet coated on the bottom with 25 μm adhesive featuring holes to permit the passage of tubing to connect the off-card syringe pumps and valves. The device layers were registered and assembled on an alignment jig (neither the alignment pins nor holes are shown for clarity). The adhesive was secured by pressing the assembled layers at 2000 p.s.i. for ~10 seconds using a hydraulic press (ICL, Garfield, NJ). The patterned surfaces and devices constructed using this method were relatively straight forward and inexpensive to produce. This, combined with the uncertainties associated with "regenerating" a used sensor surface and the need to avoid cross-contamination between samples, motivated us to use each device only once; at the present time we have not investigated their potential for re-use.

Fluid control

Fluid flow was controlled using a custom-built "microFlow" workstation (Micronics, Inc Redmond, WA) fitted with 64 μl pump barrels. All pumps shared a common upstream reservoir filled with buffer (Dulbecco's phosphate buffered saline (PBS)). The outlet of each pump was connected to a manual six-port injection valve (Upchurch Scientific, Oak Harbor, WA) via 1/16" OD, 0.03" ID PEEK tubing. Sample loops (100 μl each) were installed on each injection valve in a first-in, last-out configuration. The microfluidic device was connected to the injection valves via a short length of tubing as illustrated in Figure 2.

SPR image acquisition

The image data were collected using a custom-designed miniature SPR imaging instrument[10]; this was operated at 880 nm using LED illumination and a BK7 glass prism for coupling incident photons to surface plasmons. The detector was an 8-bit 640 × 480 charge-coupled device (Vision Components, GmbH, model VCSBC4018). For the experiments described herein, the CCD array's digital signal processor (DSP) hardware was set to integrate each image for 20 ms. The DSP co-added 30 images before delivering the summed frame to the data analysis computer. The average pixel intensity values were calculated at run-time using custom-written code (Labwindows/CVI, National Instruments, USA) by multiplying by summed pixel values by 128, converting the data into 2-byte signed fixed-point format, then dividing the pixel values by the number of co-added images. In this way, the 8 bit data from the CCD chip were transformed onto a 16-bit data range. Prior to each experiment, the incident angle of the LED was positioned to set the reflectivity value of the BSA-phenytoin region to ~30% (at the bottom of the linear range of the SPR curve[32]). An initial image was taken before the start of the experiment; this image was subtracted from subsequent images to highlight the changes in reflectivity that occurred during the course of the assay.

Assay implementation

The reader will recall that the CGIA method compares the distribution of antibody binding on the SPR sensing surface to the interfaces between the fluid streams and correlates any difference to the concentration of analyte in the sample (Figure 1). Therefore, each experimental run used to obtain data presented below was conducted in two phases: 1) a device calibration phase, used to determine the fluid interface positions, and 2) the assay execution phase. The "assay shift" was determined by comparison of the outcomes of the two phases. Each phase is conducted as follows.

Device calibration—In principle, the two fluid interfaces would trisect the width of the channel. Locating them would be a simple matter of determining the pixel positions of the channel walls and calculating which pixels were imaging the interfaces. In practice, however, the ablative cutting process used to create the channel walls necessarily generates uncontrolled surface roughness with radii of roughly 10 μm. These rough edges sometimes conspired to nucleate bubble formation during the course of an experiment, often at the position of the PEG / BSA-conjugate interface. Any significant bubbles (i.e., with a size greater than the pixel resolution) would narrow the channel width and therefore change the position of the interface. As will be detailed below, accurate knowledge of the interface locations is critical to the development of a precise assay metric. Therefore, to account for potential variations from their theoretical location, a method was developed to empirically determine the positions of the fluid interfaces in a given device prior to conducting an assay. This was accomplished by flowing water into the center inlet of a channel filled with buffer while flowing buffer into the outer two inlets. Because SPR responds to bulk refractive index changes, this resulted in a sharp drop in SPR intensity in the areas of the sensor surface in contact with water. The fluid boundaries were identified as those pixels with intensity values halfway between the average intensities of the center and outer "thirds" of the channel.

Identifying these locations was carried out as follows. First, the leading edge of the BSA-phenytoin region was identified, and the image position ~10 pixels downstream of this location orthogonal to the fluid flow direction was selected by the experimentalist. (The actual position of the leading edge was not used as patterning artifacts were often observed there, leading to difficulties in data processing). These two points defined a line across the image used as the center of a line intensity profile 5 pixels wide calculated for each frame collected over the course of the experiment. A software algorithm scanned the line profile data from ends inward to determine the average baseline (in the outer thirds) and minimum SPR intensity values (in the channel center). Fifty pixels in each region were used to determine the average baseline and minimum values. The mean value between the baseline and minimum defined the position of the fluid interface.

Assay execution—To conduct the assay, the channel was refilled with buffer, and the sample loops were filled with the following solutions: anti-phenytoin monoclonal antibody (Fitzgerald Industries International, Inc., 100 nM in PBS) in the center channel, a solution of phenytoin (Sigma, in PBS, concentrations as indicated) in the left channel, and the right loop filled with buffer as a control. The assay was initiated by starting flow (30 nL/sec) in all three fluid streams, delivering the analyte in the left stream but withholding the antibody from the center stream (the pumps delivered buffer instead.) This proceeded for ~45 seconds to allow the fluid flow to stabilize and a steady-state transverse analyte concentration gradient to form. At that point the valve controlling the antibody solution was switched to deliver the antibody into the center stream of the channel. The resulting accumulation of antibody to the surface was monitored using SPR intensity difference imaging.

Assay Quantitation—Following antibody deposition, the 50% intensity location process was repeated, but instead of a minimum value in the center of the channel, antibody adsorption led to an increase in SPR intensity; locating the positions of mean intensity between baseline and maximum values determined the "edges" of the antibody band. The positions of the fluid interfaces were compared with the edges of the antibody band; the difference between the fluid interface and the edge of the antibody band on the sample side of the channel was defined as the "assay shift" and calculated in microns.

RESULTS

Figure 4 shows a SPR difference image illustrating the essential features of the CGIA assay. In this example, 400 nM phenytoin in PBS was injected into the left stream, 75 nM anti-phenytoin antibody in PBS in the center stream, and PBS alone into the right stream. The difference data in Figure 4 highlights the changes reflected intensity that occurred as a result of antibody binding. The bright band in the center of the image is the area where antibody accumulated over the 10-minute time course of the experiment. The horizontal dotted lines delineate the regions of the channel occupied by the buffer calibration streams (calibration image data not shown). Note that the edge of the antibody band in the image coincides with the control interface, whereas the edge of the antibody band on the competitor side is shifted 36 pixels (~500 μm) into the antibody stream relative to the position of the sample interface.

Figure 5 compares line intensity profile data for the water calibration and assay execution phases of the example experiment shown in Figure 4. The vertical axes in Figure 5 have been scaled to the data range for both the assay (left axis) and water calibration (right axis) so that the positions of half-maximum intensity can be compared. As expected, the position of the control interface determined using this method coincides with the edge of the bound antibody region, whereas there is a significant difference between the position of the sample interface and the antibody edge on the competitor side of the antibody stream. Because of the steady-state distribution of antibody / analyte complex transverse to flow, the position of this interface does not change significantly over time (data not shown). At this antibody concentration, sufficient signal was obtained after 10 minutes to consider the assay complete.

Using this method, the assay shift was determined using a range of competitor concentrations and 100 nM anti-phenytoin antibody. This dependence is shown in Figure 6. When using this antibody concentration, the assay shift is approximately linear over a range of competitor concentrations from 0 to at least 300 nM; however, a full three-dimensional multiphysics computational model of this method as been completed[25], and shown to be in excellent agreement with the experimental data over the range of analyte concentrations measured (Figure 6). We note that under the described conditions, the assay shift plateaus at high analyte concentrations. This results from the non-linearity of the diffusion-based concentration gradient at distances far from the interface between the fluid streams. A corollary of this is that the assay shift dependence is a function of the retention time in the channel; slower flow rates or greater distances downstream would allow for greater diffusion of the analyte into the antibody stream, broadening the assay shift dependence and the linear dynamic range of the assay.

DISCUSSION

Multiple, dynamic mass transport and molecular binding processes occur during the execution of this assay, including pressure-driven fluid flow, molecular diffusion, antibody-antigen binding (both in solution and to the sensor surface), and near-sensor surface antibody depletion. All these processes occur simultaneously and involve spatial and temporal dependences. Because of the relative complexity of this assay method, compared, for example, to an indirect

competitive immunoassay carried out using a 96-well plate, we have developed a detailed, three-dimensional multiphysics computational model to help elucidate the important reaction mechanisms and provide insight into data interpretation and assay optimization. The results of this model are presented and discussed in a companion paper (see 25).

This assay method offers several substantial improvements over indirect immunoassay methods performed using standard 96 well plates. For instance, this assay method is quite rapid, providing signal well above detector noise in less than 10 minutes using off-card valves and sample loops. Because of the relatively low flow rates used (30 nL/sec), having the sample loops external to the microfluidic device contributes significantly to the time required to complete an assay. Thus, the time required could be substantially reduced by incorporating the valves and sample loops onto the device. Doing so would also reduce the amount of sample required to complete the assay. An additional benefit is that the antibody binding is detected directly, eliminating the need for expensive, labeled reagents, or time-consuming washes and development steps.

The dynamic range of this assay method is determined by different factors than typical indirect competitive immunoassays[33, 34]. These assays are usually performed by immobilizing an antigen analog to the surface of a substrate and then exposing the functionalized surface to a mixture of labeled antibody and sample containing the analyte. After allowing a defined time to elapse for antibody binding, the substrate is washed and the amount of bound label quantified. The useful dynamic range of this type of assay is determined by the concentration of antibody (and thus the number of antibody binding sites) used. Assuming a high-affinity antibody is available, the linear range of the assay will be approximately centered around the point of equivalence, i.e., the analyte concentration that is equal to the concentration of antibody binding sites. Much lower analyte concentrations than this will not significantly reduce antibody binding, and much higher analyte concentrations will simply block all antibody binding.

In comparison, because the method described herein relies on the diffusion of analyte a distance into the antibody stream, the analyte concentration could be significantly higher than the antibody concentration (i.e. far from equivalence), yet the geometry of the method will still allow detectable antibody surface binding along the channel at distances far enough away from the interface that the steady-state concentration of analyte is near the equivalence point. At locations closer to the interface all antibody binding will be inhibited, while at distances further from the interface, antibody will bind to the surface unimpeded by the presence of analyte in the sample.

The assay method described herein can be readily adapted for simultaneously assaying multiple analytes in a single sample. This can be accomplished by patterning stripes of different antigens across the SPR sensor surface transverse to the convective flow direction and including additional (non-cross reacting) antibodies to those antigens in the center stream. The diffusion of the different analytes in the sample stream into the antibody-containing stream followed by binding to the spatially-addressed surface bound antigen would enable the simultaneous quantitative detection of each analyte in the sample.

CONCLUSIONS

We have demonstrated a novel microfluidic competitive immunoassay format that allows immunoassays for low molecular weight analytes in less than 10 minutes using a ~20 μL fluid sample and SPR imaging detection, on an inexpensive, single-use microfluidic device. No mixing of fluids (other than that which occurs by diffusion in the device) is required. This method is suitable for rapid immunoassay detection of low molecular weight analytes in a point-of-care diagnostic system.

ACKNOWLEDGEMENTS

The authors gratefully acknowledge funding from the National Institute of Dental and Craniofacial Research (5U01 DE014971-03). We also would like to thank Drs. Timothy Chinowsky and Michael Grow for significant contributions to the development of the SPR imaging system used in this report and also to Dr. Thayne Edwards for the implementation of the o-ring device interface described herein. Finally, we gratefully acknowledge Dr. Elain Fu for her capable oversight of this research effort.

REFERENCES

1. Yager P, Edwards T, Fu E, Helton K, Nelson K, Tam MR, Weigl BH. Nature 2006;442:412–418. [PubMed: 16871209]
2. Castner DG, Ratner BD. Surface Science 2002;500:28–60.
3. Rich RL, Myszka DG. Current Opinion in Biotechnology 2000;11:54–61. [PubMed: 10679342]
4. Homola J, Yee SS, Gauglitz G. Sensors and Actuators B-Chemical 1999;54:3–15.
5. Knoll W. Annual Review of Physical Chemistry 1998;49:569–638.
6. Schuck P. Annual Review of Biophysics and Biomolecular Structure 1997;26:541–566.
7. Janata J, Josowicz M, Devaney DM. Analytical Chemistry 1994;66:R207–R228.
8. Malmqvist M. Current Opinion in Immunology 1993;5:282–286. [PubMed: 8507407]
9. Vadgama P, Crump PW. Analyst 1992;117:1657–1670.
10. Chinowsky T, Grow M, Johnston K, Nelson K, Edwards T, Fu E, Yager P. Biosensors & Bioelectronics. 2006in press
11. Whitesides GM. Nature 2006;442:368–373. [PubMed: 16871203]
12. Weston AD, Hood L. Journal of Proteome Research 2004;3:179–196. [PubMed: 15113093]
13. Erickson D, Li DQ. Analytica Chimica Acta 2004;507:11–26.
14. Sia SK, Whitesides GM. Electrophoresis 2003;24:3563–3576. [PubMed: 14613181]
15. Hansen C, Quake SR. Current Opinion in Structural Biology 2003;13:538–544. [PubMed: 14568607]
16. Weigl BH, Bardell RL, Cabrera CR. Advanced Drug Delivery Reviews 2003;55:349–377. [PubMed: 12628321]
17. Beebe DJ, Mensing GA, Walker GM. Annual Review of Biomedical Engineering 2002;4:261–286.
18. Schulte TH, Bardell RL, Weigl BH. Clinica Chimica Acta 2002;321:1–10.
19. Becker H, Locascio LE. Talanta 2002;56:267–287. [PubMed: 18968500]
20. Stone HA, Stroock AD, Ajdari A. Annual Review of Fluid Mechanics 2004;36:381–411.
21. Kaufman E, Lamster IB. Critical Reviews in Oral Biology & Medicine 2002;13:197–212. [PubMed: 12097361]
22. Malamud D. Journal of the American Dental Association 2006;137:284–+. [PubMed: 16570454]
23. Wong DT. Journal of the American Dental Association 2006;137:313–321. [PubMed: 16570464]
24. Mandel ID. Journal of the American Dental Association 1993;124:85–87. [PubMed: 8445148]
25. Foley J, Nelson K, Mashadi-Hossein A, Findlayson B, Yager P. Analytical Chemistry. 2006Submitted
26. Hatch A, Kamholz AE, Hawkins KR, Munson MS, Schilling EA, Weigl BH, Yager P. Nature Biotechnology 2001;19:461–465.
27. Kamholz AE, Weigl BH, Finlayson BA, Yager P. Analytical Chemistry 1999;71:5340–5347. [PubMed: 10596213]
28. Jung LS, Campbell CT, Chinowsky TM, Mar MN, Yee SS. Langmuir 1998;14:5636–5648.
29. Prime KL, Whitesides GM. Journal of the American Chemical Society 1993;115:10714–10721.
30. Creighton, TE. Proteins: structures and molecular properties. Second edition. W. H. Freeman; New York: 1993.
31. Malamud, D.; Tabak, LA., editors. Saliva as a diagnostic fluid. New York Academy of Sciences; New York: 1993.
32. Shumaker-Parry JS, Campbell CT. Analytical Chemistry 2004;76:907–917. [PubMed: 14961720]
33. Knecht BG, Strasser A, Dietrich R, Martlbauer E, Niessner R, Weller MG. Analytical Chemistry 2004;76:646–654. [PubMed: 14750859]

34. Li Y, Kobayashi M, Furui K, Soh N, Nakano K, Imato T. Analytica Chimica Acta 2006;576:77–83. [PubMed: 17723617]

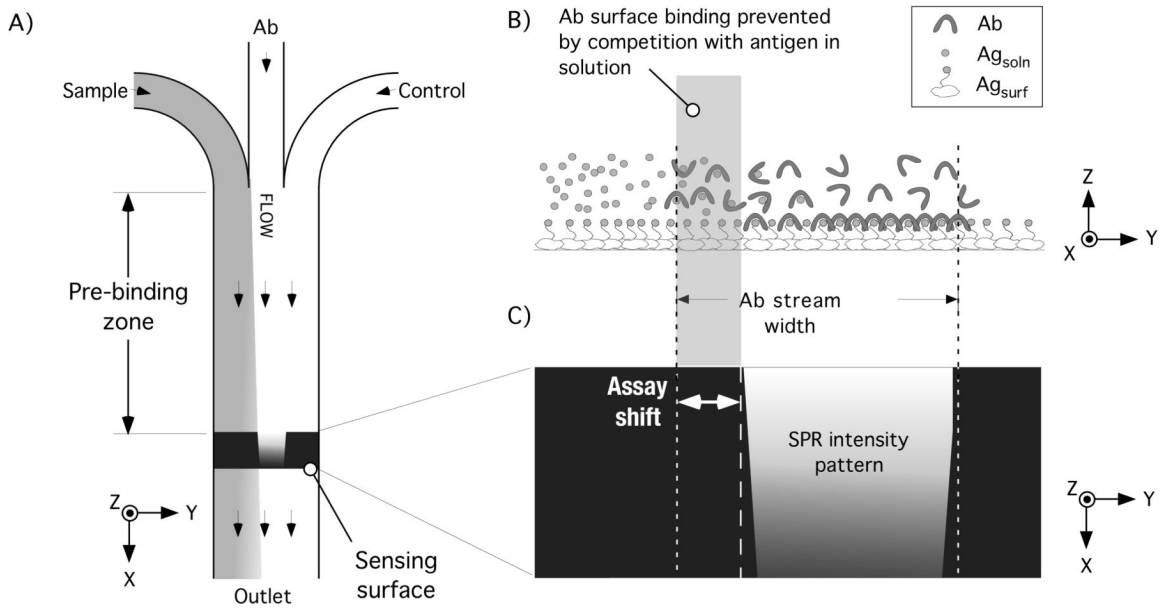

Figure 1. Schematic overview of the concentration gradient immunoassay method

A) Device geometry (not drawn to scale). Three fluid inlets streams converge within a single channel: one containing the analyte of interest (sample), one containing an antibody against the analyte, and (optionally) a reference or control stream. Following convergence, the fluids flow down a channel for some distance to permit diffusive mass transport among the fluid streams. This portion of the channel surface is functionalized with PEG to resist protein adsorption. After interdiffusion establishes a gradient of antibody / analyte complexes transverse to flow, the fluids then encounter the sensing surface that is functionalized with surface-bound analyte. B) Schematic view of competition between solution-phase analyte and surface-immobilized analog for antibody binding sites. Diffusion of solution-phase analytes into antibody stream establishes gradient of occupied antibodies. Only antibodies with at least one open binding site may bind to surface, leading to an SPR signal change. View is through channel from outlet. C) Cartoon of SPR difference image obtained after antibody accumulation to the sensing surface. The “assay shift” is the difference between width of the center flow stream and the region of the surface that antibodies accumulate onto. Axes indicate view direction: +x is through the channel in the direction of fluid flow.

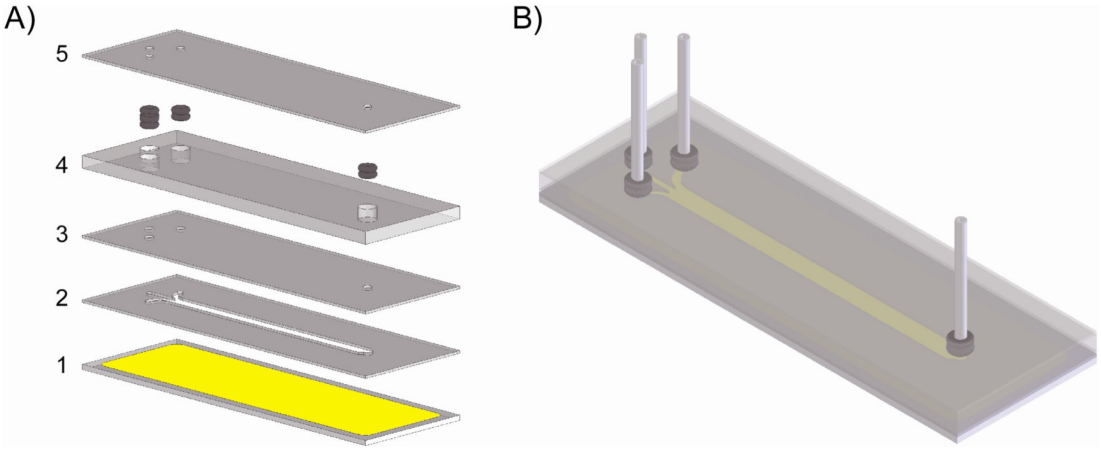

Figure 2.

Microfluidic assay device and assembly. Exploded view (A) shows layers used (from bottom to top): 1) Substrate, a soda-lime glass 75 mm × 25 mm microscope slide coated with 4.5 nm gold on its upper surface, this gold surface is functionalized prior to device assembly (see text); 2) Channel, a 12 μm Mylar™ sheet coated on both sides with 25 μm pressure-sensitive adhesive to produce a channel 62 μm in depth; it features a 3.6 mm channel laser-cut from center with three inlets and a single outlet; 3) Device cap, a 25 μm Mylar™ layer (with adhesive on top only) with vias to permit fluid flow; 4) O-ring seat, a 2.5 mm PMMA layer with laser-cut holes for EPDM O-rings; 5) O-ring retainer, a 25 μm Mylar™ layer (adhesive on bottom) with laser-cut holes to pass tubing. (B) Rendering of assembled device and tubing (pumps, valves, and waste reservoir not shown).

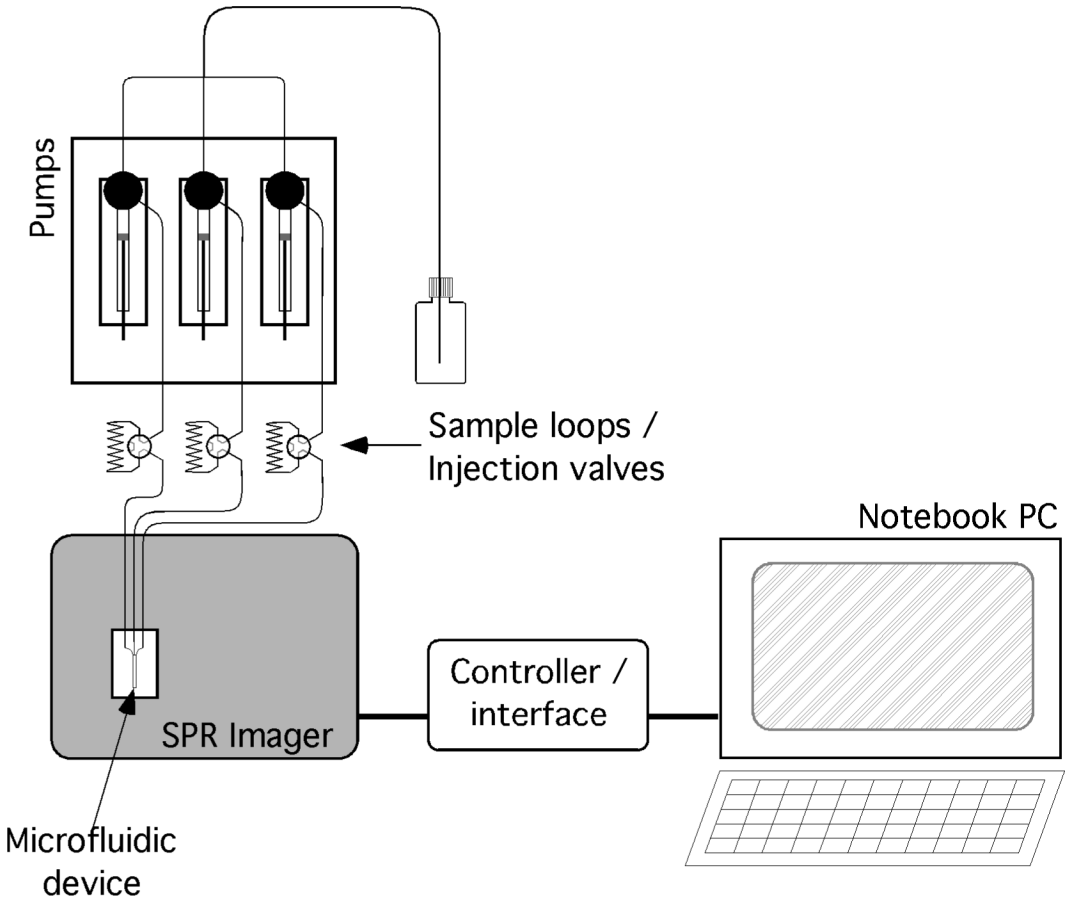

Figure 3.

Schematic diagram of experimental apparatus. The SPR mini imager is operated with a notebook computer interfaced to the instrument via custom fabricated control hardware driving the LED angle position controller, LCD polarizer, and camera / DSP hardware[10]. The microfluidic device is refractive index-matched to the imaging prism and connected via PEEK tubing to off-card sample loops, injection valves, and syringe pumps fed from a common buffer reservoir.

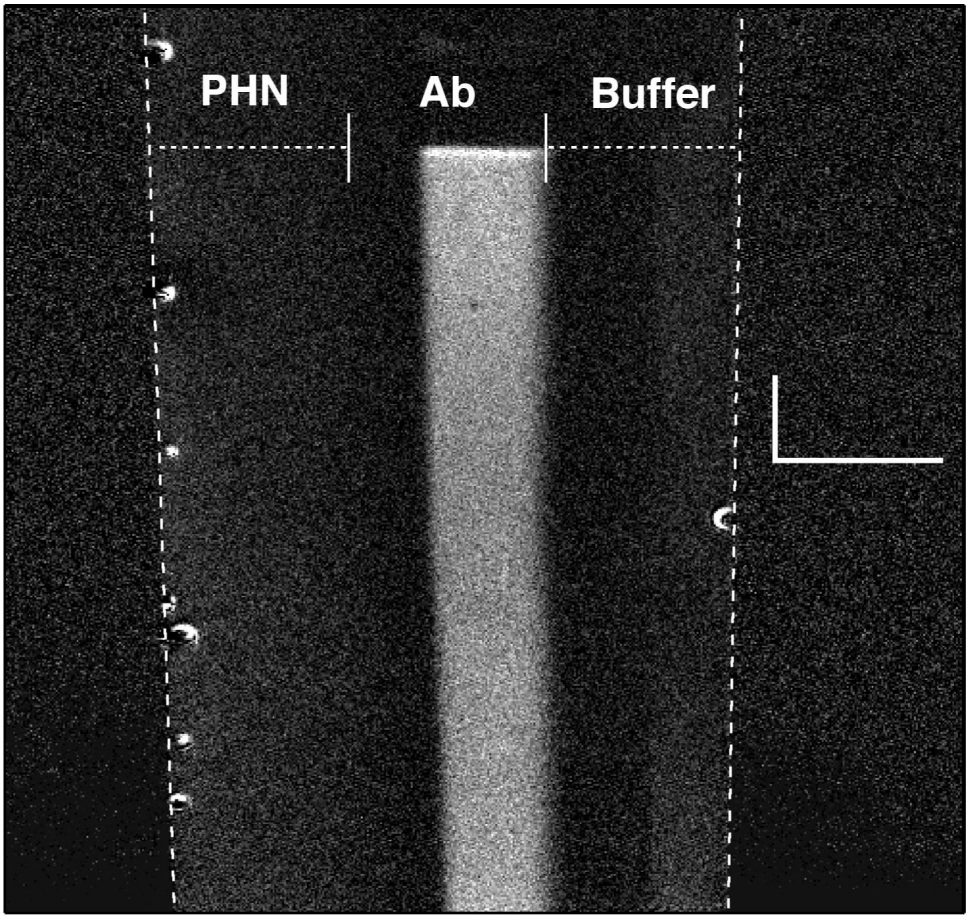

Figure 4.
SPR difference image illustrating assay result. All three fluids are PBS containing the indicated solutes: 400 nM phenytoin (PHN) on the left, 75 nM anti-phenytoin antibody (Ab) in the center, buffer only on the right. The total volumetric flow rate was 90 nL/sec (30 nL/sec/inlet) from top to bottom. The image elapsed time is 600 seconds. The vertical dashed lines are shown to highlight the channel edges. The horizontal dashed lines and short vertical bars delineate the approximate width of the two outside fluid streams as well as the position of the PEG thiol / BSA-phenytoin surface pattern interface. The scale bars (outside the channel region, center right) are 1 mm each. Note that apparent convergence of parallel channel walls due to optical keystone artifacts. The contrast in the image has been scaled to data value range (see Figure 5).

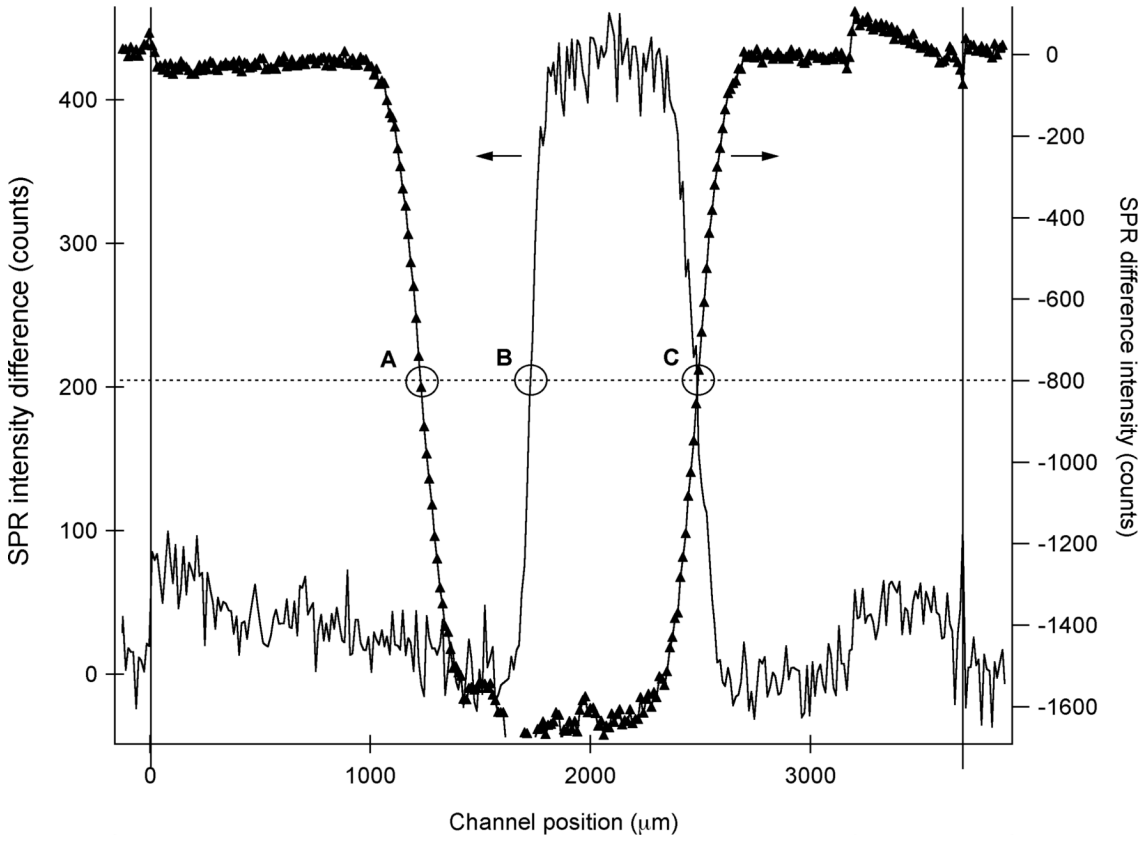

Figure 5.

Intensity line profile comparison between width of center fluid stream and surface antibody distribution following concentration gradient immunoassay. The position of the fluid interfaces for a given device were empirically determined by flowing buffer, water, and buffer into the left, center, and right inlets (respectively) of a device previously filled with buffer (triangles). The refractive index difference between water and buffer led to a sharp drop in SPR image intensity. Shown in comparison is the SPR image intensity profile (solid line) obtained from a concentration gradient assay run using 400 nM phenytoin in the left stream, 75 nM anti-phenytoin antibody in the center stream, and buffer alone in the right stream (solid line) after 600 seconds. Note that the 50% maximum intensity points at ~420 pixels are aligned (C); the significant shift is apparent between the calibrator (A) and the data curve (B). Arrows indicate corresponding data axes, solid vertical lines indicate channel edge positions.

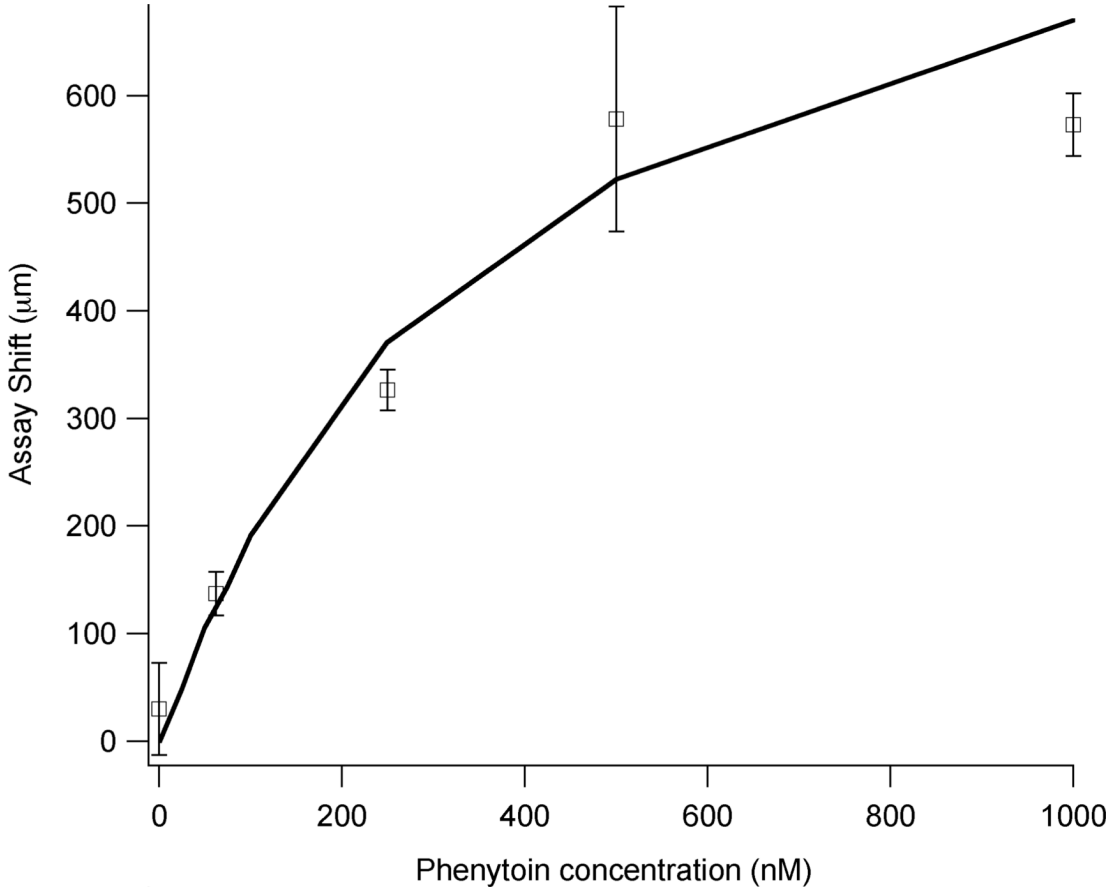

Figure 6.

Assay shift dependence (in microns) vs. analyte concentration. Points represent average values (± 1 standard deviation ($n \geq 3$)) obtained using indicated analyte concentrations in the sample stream adjacent to a 75 nM antibody solution. The black line represents the assay shift calculated using a computational model that solves Navier-Stokes fluid flow, convection-diffusion, and solution and surface binding in three dimensions (see Foley et al. [25]) for the device geometry used in these experiments.